EXPERIMENTAL STUDY OF THE HEAT TRANSFER ENHANCEMENT BY CORONA WIND IN A SQUARE CHANNEL

Havet M.* and Ould Ahmedou S.A.
*Author for correspondence
Laboratory of Process Engineering for Environment and Food,
ONIRIS
Rue de la géraudière,
44322 Nantes,
France,
E-mail: michel.havet@oniris-nantes.fr

ABSTRACT

Convective heat transfer is still the major heat transfer mode in bio and food processes where air is commonly used as the heat transfer medium. Alternative processes should be investigated in order to enhance heat transfer. This work concerns the ElectroHydroDynamic (EHD) enhancement of the convective heat transfer in a square channel. An experimental set-up was designed in order to determine the local heat transfer coefficient at the surface of a heated plate. Conditioned air (controlled temperature and humidity) was introduced in a square channel at a velocity ranging from 0 to 5 m/s. A corona electrode was placed in the channel in order to generate an ionic wind. The applied voltage was ranging from 0 to 20 kV. An infrared camera was used to measure the surface temperature of the heated plate at the bottom surface of the channel. This original experimental device was used to determine the local heat transfer coefficients for different configurations (various inlet air velocities and applied voltages). Results showed that the electrical body force and the inertial force had synergetic effects for low Reynolds number. It was demonstrated that the corona wind could lead to a fourth increase of the mean heat transfer coefficient. Nevertheless, at higher Reynolds number, the corona wind had no more effect on the heat transfer.

INTRODUCTION

Forced convective heat transfer is the main heat transfer mode in bio and food processes. Air is widely used in heating or refrigerating processes despite its bad heat transfer properties. To ensure the desired treatments, high velocities are required and lead to high energy consumption. The boundary layers that form on the surfaces offer a significant resistance to the flow of heat. Enhancing techniques should therefore be performed in order to modify the air flow and to increase the convective heat transfer coefficient. The Electrohydrodynamic (EHD) enhancement technique offers a great potential. Allen and Karayiannis [1] mentioned that the "corona wind" could enhance single phase convective heat transfer. The corona wind is produced at the vicinity of a highly curved electrode surface where the local electric field strength is sufficiently large to ionize the gas molecules [2]. The ionization zone remains localized around the corona electrode. While the whole process is rather complex [3], the net effect is that ions of the same polarity as that of the corona electrode, are drifting to a collector electrode. Outside the ionization zone is the region called the drift zone where momentum is transferred, by collision, from the ions to the neutral air molecules. The resulting flow has been termed the corona wind [3, 4]. The EHD enhancement of heat and mass transfer by corona wind, so-called corona discharge, has been extensively studied in external boundary layers or free convection systems. The EHD enhancement of heat and mass transfer in natural convection was clearly demonstrated by Owsenek and Seyed-Yagoobi [5]. Concerning the enhancement of heat transfer in the case of forced convection, contradictory results were observed for a laminar tangential flow over a surface. Sadek, Fax and Hurwitz, showed that the combined effect of inertia and electrical force could lead to a four-fold increase of the Nusselt number [6]. Other authors observed no enhancement of heat or mass transfer by EHD [7]. Literature is rather poor concerning the EHD enhancement of heat transfer in channel flows. Most of them concerned a wire electrode parallel to the main air flow for heat exchanger applications [8, 9]. They revealed that the corona induced secondary flows that enhanced heat transfer in both fully-developed and developing regions. The case of a transversal electrode in a channel received less attention despite its great interest in bio and food processes [10, 11].

This experimental work concerns the influence of the ionic wind on the local heat transfer coefficient at the surface of a heated plane in a square channel. The experimental set-up and

the methods are firstly described. In a second stage the experimental results are presented for a positive applied voltage of 15 kV. Finally, the influence of both the inlet velocity and the applied voltage on the heat transfer is discussed.

NOMENCLATURE

A	[m²]	Area
b	[m²/V/s]	Ion mobility
d	[m]	Inter-electrode distance
D	[m]	Diameter
D_h	[m]	Hydraulic diameter
E	[V/m]	Electric field strength
Ec	[V/m]	Electric field of ionization
EF	[-]	Enhancement Factor
h	[W/m²/K]	Convective heat transfer coefficient
H	[m]	Channel height
I	[A]	Electric current
J	[A/m²]	Current density
L	[m]	Channel depth
N_{EHD}	[-]	Electric number
Nu	[-]	Nusselt number
Re	[-]	Reynolds number
R	[m]	Radius
R_c	[m]	Radius of ionization zone
T	[°C]	Temperature
U	[m/s]	Air velocity
V	[V]	Voltage
x	[m]	Cartesian axis direction
y	[m]	Cartesian axis direction
z	[m]	Cartesian axis direction

Special characters

λ	[W/m/K]	Thermal conductivity
Γ	[m²/s]	Ion diffusivity
ρ	[kg/m³]	Density of air
ρ_c	[C/m³]	Ion charge density
ν	[m²/s]	Kinematic viscosity
φ	[W/m²]	Heat flux

Subscripts

e	Electric
EHD	With EHD
$noEHD$	Without EHD
p	Heated plate
w	Wall
0	Wire electrode

EXPERIMENTAL SET-UP

The experimental setup used in this investigation is shown in Figure 1. Air, at controlled temperature (20°C) and humidity (20 %), was blown at the desired velocity U_{in} [0-5 m/s] in a square channel (15x15 cm). The channel, made of polyurethane material (thickness 2 cm) was 2 m long and the test section was located at 1.5 m from the entry. We verified that the flow was fully developed at x/D_h=10. A high-voltage DC power supply was used to charge the wire electrode (R_0=0.1 mm). The temperature profile of the plate was measured with an infrared camera. The air temperature and the temperature of the walls close to the test section were measured using K-type thermocouples. As shown in Figure 2, a sapphire window was used to permit the surface temperature measurement without perturbation of the airflow. The disk of sapphire (diameter equal to 9 cm) was transparent in the wavelength range 3-5 μm

corresponding to the infrared camera. A data acquisition system was used to record the different measurements. Another power supply was used for the heated plate shown in figure 3. It was constituted of very thin layers of conductive and dielectric materials. The upper copper layer was used as the ground electrode. The plate surface was lightly painted homogeneously to diminish the shining surface of the copper. The emissivity of the plate surface was determined from accurate temperature measurements of the plate temperature to yield a value of 0.99. The infrared camera was calibrated before every set of experiments. The sensitivity of the camera was ±0.1°C with a spatial resolution of 0.428 mm/pixel. The temperatures were measured at the centre line of the heated plate (along a line perpendicular to the wire) so that edge effects were not included in the subsequent calculations. The non-isothermality of the plate parallel to the wire direction was found equal to 0.2°C; it was of the same order than the sensitivity of the camera.
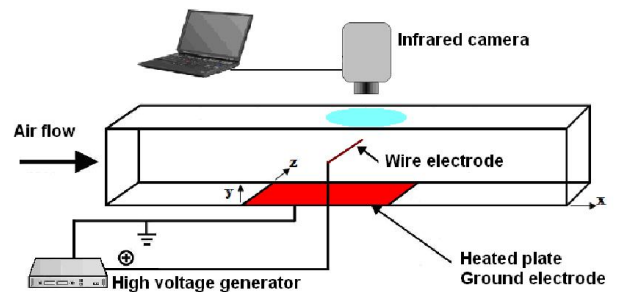

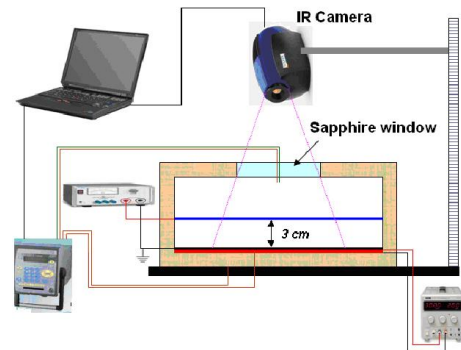**Figure 1** Sketch of the experimental bench (general view)

Figure 2 Sketch of the experimental bench (side view)
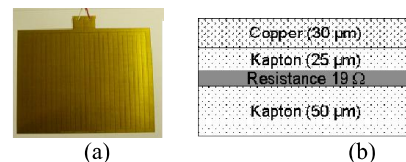

(a)   (b)
Figure 3 Heated plate
(a) photo before painting   (b) scheme of the layers

EXPERIMENTAL RESULTS

All the experiments were conducted with a wire located at 3 cm above the heated plate. This inter-electrode distance was selected from previous numerical simulations [10, 12]. At the test section, the flow field was fully developed whereas it was thermally developing.

Current-Voltage characteristics

Before conducting heat transfer experiments, air velocity, temperature and humidity were recorded to verify their stability. Moreover, the stability of the high voltage source was verified. The positive applied voltage V_0 was incrementally increased from 4 to 20 kV and the corona current was measured. In a second stage, a similar experiment was conducted by decreasing the voltage. The resulting Current-Voltage characteristics are shown in Figure 4. It is noticeable that, contrary to other experimental results in the literature, no hysteresis was observed. This is probably due to the better control of the ambient conditions, especially the air humidity. In this configuration, the onset voltage is close to 9 kV; ionization of air appears at this value and ions are drifted towards the ground plate. In the following heat transfer experiments, the applied voltage was set at 15kV.
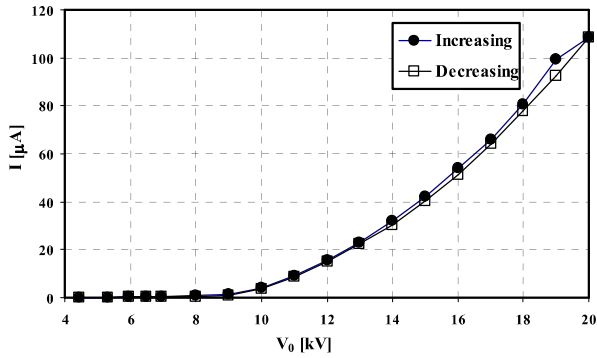

Figure 4 Current-Voltage characteristics obtained by increasing or decreasing the voltage

Heat transfer measurements (V_0=15kV)

In the heated plate, we fixed the current at 0.4 A and the voltage was 6.8 V. The corresponding electric power was entirely dissipated by Joule effect ($\varphi_{heating}$ = 121 W/m²). Figure 5 illustrates the heat losses by conduction throughout the polyurethane, by radiation with the internal walls of the channel and by convection with the flowing air.
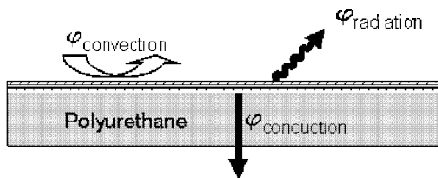

Figure 5 Heat flux distribution

The stationary regime was quickly obtained (less than 10 minutes). In these conditions, a simple heat balance can be expressed by equation 1. The radiative heat flux was determined by considering that the walls of the channel were at

the air temperature. Equation (2) permits to calculate the local convective heat transfer coefficient by assuming a constant mean air temperature. This assumption was verified by measurements at different location in the channel. Once the heat transfer coefficient was determined at a given Reynolds number (equation 3), the local Nusselt number was obtained from the conventional definition (equation 4). In a square channel the hydraulic diameter D_h is equal to the height of channel H.

$$\varphi_{convection} = \varphi_{heating} - \varphi_{conduction} - \varphi_{radiation} \quad (1)$$

$$h_x = \frac{\varphi_{convection}}{T_{w,x} - T_{air}} \quad (2)$$

$$Re = \frac{U_{in} D_h}{\upsilon} \quad (3)$$

$$Nu_x = \frac{h_x D_h}{\lambda_{air}} \quad (4)$$

Experiments were performed at 15 kV for inlet velocities ranging from 0 to 1.25 m/s. Table 1 indicates the corresponding Reynolds numbers and how the generated heat flux was evacuated. A natural convection case (U_{in} =0) was considered only to get a reference for comparison with forced convection cases. In these experiments, convection represented between 68 and 80% of the generated heat flux. It means that in these conditions, convection was predominant; the heat transfer with the air was good but radiation could not be neglected. It is amazing to note that the lower convective part was obtained at the higher Reynolds number. Moreover, it was close to that obtained in the natural convection case. These preliminary results confirmed that the corona discharge could generate a relatively high convective heat flux.

Table 1: Relative part of the generated heat flux (V_0=15kV)

U_{in} [m.s^{-1}]	Re [-]	conductive heat flux [%]	radiative heat flux [%]	convective heat flux [%]
0	/	3.6	24.6	71.8
0.2	1920	0.1	20.3	79.5
0.56	4941	0.1	24.7	75.2
1.25	11127	3.0	28.8	68.2

For the natural convection case and the higher Reynolds case (1.25 m/s), the corresponding plate temperatures issued from the infrared camera are presented in figure 5 and 6 respectively. The vertical line in these figures corresponds to the shadow of the wire. It just permitted to know its location. The horizontal line #1 is the centre line where temperature was extracted for calculation. It should be firstly mentioned that in natural convection without electric field, the plate temperature was initially equal to 37.5 ±0.2°C. These pictures permit to get an idea of the location where the cooling effect is predominant. They also demonstrate that in this experimental set-up, the heat transfer could be considered as one dimensional. It is perfectly

observed in the natural convection case depicted in figure 6. There was no temperature gradient in the trans-wise direction. The corona wind acted like an impinging jet with a higher heat transfer rate just below the wire. On figure 7, there was an interaction between the airflow incoming from the left side and the ionic wind. The temperature distribution was very different with a higher cooling of the plate on the right side of the plate. A deeper analysis of the temperature profiles is required to discuss this phenomenon.
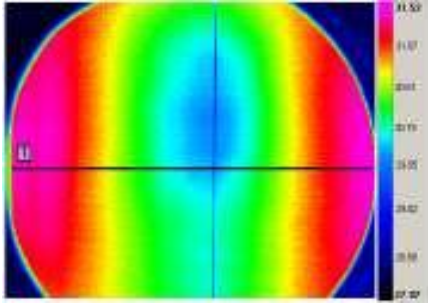

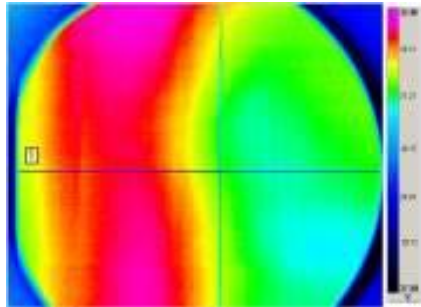**Figure 6** Surface temperature recorded by IR camera, $V_0 = 15$kV, $U_{in} = 0$ m/s

Figure 7 Surface temperature recorded by IR camera, $V_0 = 15$kV, $U_{in} = 1.25$ m/s, Re=11127 (Airflow from the left to the right)

Figure 8 presents the temperature evolutions along the heated plate for two inlet velocities, 0.56 and 1.25 m/s, with or without ionic wind. The corresponding local heat transfer coefficients calculated using equation 2 are depicted on figure 9. The cases without electric field correspond to pure force convection. In these conditions, the incoming flow field was fully developed. As expected, we observe on figure 8 that without electric field ($V_0=0$), the cooling of the plate by the air was the greatest for the higher inlet velocity. The cooling was also more efficient at the leading edge of the plate. These typical pure forced convection cases are also shown on figure 9. It clearly appears that the local heat transfer coefficient is linked to the inlet velocity. It should also be indicated that we verified, but do not show in this paper, that these forced convection results agreed with correlations of the literature.

The application of the electric field ($V_0=15$kV) had a significant effect on the plate temperature. It permitted to decrease the temperature, especially for the lower inlet velocity. For $U_{in}=1.25$ m/s, the temperature distribution was modified by the ionic wind but the average temperature was not really affected. For $U_{in}=0.56$ m/s, the temperature decrease due to

ionic wind was up to 5°C below the wire. The ionic wind altered the flow field and was efficient to cool the plate. Similar trends were previously described in numerical studies [10, 12].

Figure 9 allows a discussion on the heat transfer enhancement by the electric field. At the higher velocity, the enhancement is obtained only after the wire. The value of the heat transfer coefficient increased from 10 to 15 W/m²/K. This enhancement is not really remarkable whereas it is very important at the lower velocity. In this case, a minimum of three fold increase was obtained. A maximum of four fold increased was observed at $x/L=0.5$, just below the wire electrode. This distribution of the local heat transfer coefficient is like that of an impingement jet, as described previously. It seems that the heat was mainly transferred by the ionic wind and that the air flow just served to evacuate this heat towards the outlet.
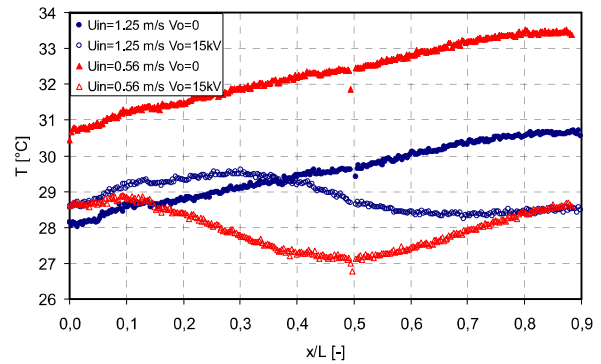

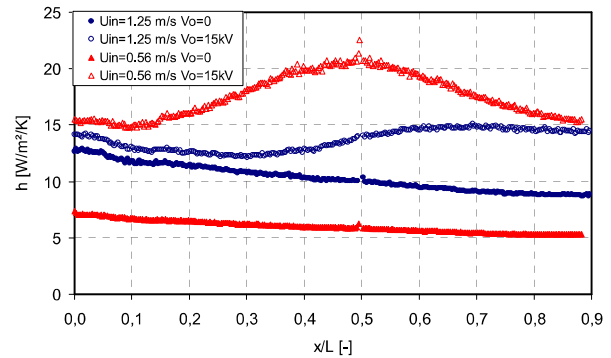**Figure 8** Temperature evolution along the heated plate

Figure 9 Local heat transfer coefficient along the heated plate

Influence of the applied voltage on the heat transfer

Other experiments were also conducted in order to analyse the influence of the applied voltage on the temperature and on the heat transfer. To allow a comparison, we defined a local enhancement factor EF_x: the ratio of the local heat transfer coefficients with and without EHD (equation 5). Experiments were previously performed to calculate the evolution of the local heat transfer coefficient without EHD, *i.e.* in pure forced

convection. A mean enhancement factor was also calculated by integration along the plate. Values of EF greater than unity indicate that the corona discharge enhances heat transfer.

Each experiment was characterized by the conventional Reynolds number (equation 3) and by the electric Reynolds number (equation 6) based on the ionic wind velocity (equation 7). The latter is deduced from the measured corona current I. The enhancement should also be related to the ratio between the electric body force and the inertial force. For this reason we also calculated the dimensionless electric number N_{EHD} (equation 6).

$$EF_x = \frac{Nu_{x,EHD}}{Nu_{x,noEHD}} = \frac{h_{x,EHD}}{h_{x,noEHD}} \qquad (5)$$

$$Re_{EHD} = \frac{U_e D_0}{\upsilon} \qquad (6)$$

$$U_e = \left[\sqrt{\frac{IL_0}{\rho b A_P}} \right] \qquad (7)$$

$$N_{EHD} = \frac{IL_0}{\rho b A_P U_{in}^2} \qquad (8)$$

The following results were obtained for two inlet velocities U_{in} (0.56 and 1.25m /s) corresponding to Re=4941 and 11127 respectively. Voltages ranging from 10 to 18 kV were applied and the corresponding electric Reynolds, electric number and mean enhancement factor are given in table 2. Figure 10 presents the evolution of the local enhancement factor in these different cases.

From table 2, it appears that for a given applied voltage, the electric Reynolds number depended on the incoming flow. This dependence was especially marked at 10 kV. From equations 6 and 7, it comes that this influence could be explained by a modification of the electric current by the flow field. It is known that the main mechanism of ions transport is convection by the electric field but the flow field could also contribute to this transport (equation 9).

$$J = \rho_c (bE + U) - \Gamma \nabla \rho_c \qquad (9)$$

At the lower Reynolds number, the electric number was slightly influenced by the applied voltage because the generated corona wind greatly increased due to a higher electric current. It was also confirmed that the mean enhancement factor increased with the electric parameter (V_0, Re_{EHD}, N_{EHD}). At the higher Reynolds number, it could be said that similar trends were observed but at considerably lower scale. The mean enhancement factor remained close to 1.

Conclusions derived from table 2 can be deeper analyzed through Figure 10 that provides details on these phenomena. We choose to present the local enhancement factor along the plate according to the electric number. It seemed the latter could be a good indicator as it represents the ratio of the electric body force to the inertial force. A first reading confirms the relevance of this parameter: the curves are arranged according to this parameter. The minimum local enhancement

factors were obtained for the minimum electric numbers whereas the maximum were obtained for the highest electric number. A six-fold increase of the heat transfer was locally obtained just below the wire for N_{EHD}=2.64. Nevertheless, a kind of saturation could be observed because the same enhancement was measured for N_{EHD}=4.91. It would be interesting to deduce correlations from these experimental results but no simple relationship could be obtained.

Table 2: Dimensionless parameters of the experiments

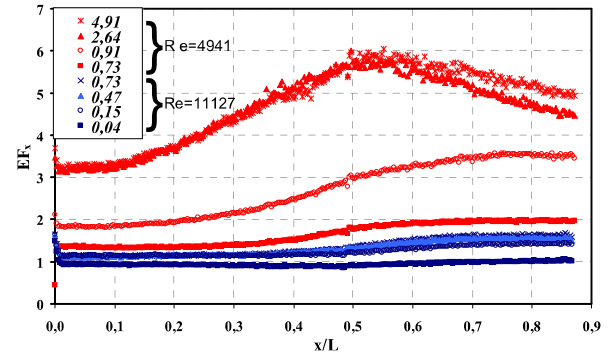| V_0 [kV]	U_{in} = 0.56 m/s Re = 4941			U_{in} = 1.25 m/s Re = 11127		
	Re_{EHD}	N_{EHD}	EF	Re_{EHD}	N_{EHD}	EF
10	6.09	0.73	1.64	3.34	0.04	0.94
12	6.81	0.91	2.67	6.09	0.15	1.23
15	11.60	2.64	4.61	10.98	0.47	1.31
18	15.83	4.91	4.73	13.63	0.73	1.34

Figure 10 Evolution of the local enhancement factor along the heated plate according to the electric number

CONCLUSION

These experiments, performed in a square channel, analysed the enhancement of the heat transfer by corona wind in a fully developed and thermally developing flow. The set-up, specifically designed for this work, was relevant to obtained accurate temperature profile and to calculate local heat transfer coefficients with and without electric field. The efficiency of the ionic wind was pointed out at Re=4941 whereas it was not interesting to apply an electric field at Re=11127. The enhancement of the heat transfer by the electric body force was demonstrated by applying, for example, 15 kV at the wire electrode. It could lead to a four-fold increase of the mean heat transfer coefficient and locally to a six-fold increase below the wire. If the dependence of the enhancement factor with the electric number N_{EHD} was well obtained, no useful and simple correlation could be proposed at this time. Further experiments should be conducted to complete the data base and to help in developing relationships that would be employed in designing EHD process based on the ionic wind. Nevertheless, the interaction between the electric body force and the inertial force

remains complex and should also be investigated by numerical approaches.

REFERENCES

[1] Allen P.H.G., Karayiannis T.G., Electrohydrodynamic enhancement of heat transfer and fluid flow, *Heat Recovery Systems and CHP*, Vol. 15, 1995, pp. 389-423

[2] Goldman M., Goldman A., Sigmond R.S., The corona discharge, its properties and specific uses, *Pure and Appl. Chem.*, Vol. 57, 1985, pp. 1353-1362

[3] Chen J., Davidson H., Electron Density and Energy Distributions in the Positive DC Corona: Interpretation for Corona-Enhanced Chemical Reactions, *Plasma Chemistry and Plasma Processing*, Vol. 22, No. 2, 2002, pp 199-224

[3] Rickarda M., Dunn-Rankina D., Weinbergb F., Carleton F. , Characterization of ionic wind velocity, *Journal of Electrostatics*, Vol. 63, 2005, pp 711–716

[4] Robinson M., Movement of air in the electric wind of the corona discharge, *AIEE Transactions,* Vol. 80, 1961, pp. 143-150

[5] Owsenek B.L., Seyed-Yagoobi J., Theoretical and experimental study of electro-hydrodynamic heat transfer enhancement through wire-plate corona discharge, *Journal of Heat Transfer*, Vol. 119, 1997, pp. 604-610

[6] Sadek S.E., Fax R.G., Hurwitz M., The influence of electric fields on convective heat and mass transfer from a horizontal surface under forced convection, *Journal of Heat Transfer*, Vol. 94, 1972, pp 144-148

[7] Lai F.C., Huang M., Wong D.S., EHD-enhanced Water Evaporation, Drying Technology, Vol. 22, No. 3, 2004, pp 597–608.

[8] Molki M., Ohadi M., Baumgarten B., Hasegawa M., Yabe A., Heat transfer enhancement of airflow in a channel using corona discharge, *Enhanced Heat Transfer*, Vol. 7, 2000, pp. 411–425

[9] Molki M., Bhamidipati K.L., Enhancement of Convective Heat Transfer in the developing region of circular tubes using corona wind, *International Journal of Heat and Mass Transfer*, Vol. 47, No. 19-20, 2004, pp. 4301-4314

[10] Ould Ahmedou S.A., LeBail A., Havet M., Influence of corona discharges on the convective heat transfer in a channel flow, *International Symposium on Advances in Computational Heat Transfer, CHT-08-320*, 2008

[11] Go D.B., Maturana R.A., Fisher T.S., Garimella S.V., Enhancement of external forced convection by ionic wind, *International Journal of Heat and Mass Transfer*, Vol. 51, 2008, pp 6047–6053

[12] Ould Ahmedou S.A., Havet M., Effect of process parameters on the EHD airflow, *Journal of Electrostatics*, Vol. 67, 2009, pp 222–227